

Acceleration of Dual Reflector Antenna Radiation Analysis using Double Bounce Physical Optics Accelerated using Multipole Method

Chunbang Wu and Jun Li

School of Electronic and Optical Engineering
Nanjing University of Science and Technology, Nanjing, Jiangsu Province 210094, China
13770328703@139.com

Abstract — The multipole method is firstly used to accelerate the radiation analysis of the dual reflector antenna with the double-bounce physical optics. The algorithm starts with physical optics to calculate the equivalent electric current on the subreflector. Then the equivalent electric current on the main reflector can be obtained through the current on the subreflector. It should be noted that the modified multilevel fast multipole method (MLFMM) is applied to accelerate the calculation between the main reflector and the subreflector. In this way, the computation complexity is reduced greatly, thus the computational time can be significantly saved. At last, numerical results are given to demonstrate the superior efficiency and accuracy of the proposed method.

Index Terms — Double-bounce physical optics, dual reflector antenna, MLFMM.

I. INTRODUCTION

Nowadays, the satellite communication has a wide application in both the military and civilian domains. The antenna technology plays a very important role in satellite communication. There are three kinds of satellite antennas, namely lens [1], phased array [2]-[3] and reflector [4]-[6] antennas. However, the weight of lens antenna is generally heavier than reflector antenna. Moreover, the phased array antenna generally need to hundreds of units in order to achieve the same gain of reflector antenna, which leads to exceed to the limit of the satellite. Therefore, the reflector antenna has a great advantage in volume and weight.

Full-wave simulation of electrically large size problems is impossible to be taken on conventional workstations due to their hardware limitations. Parallel technique provides a possibility through thousands of Giga Bytes (GB) of memory and processors connected by high-speed switches [7]. Moreover, it is an arduous task for the method of moments (MoM) for electrically large problems. In reference [8], a multi-level method based on near-field and far-field transformation of plane wave is proposed. This method uses diagonal

translation operator and is available for evaluating electrically large antennas. In [9], it presents the multilevel fast multipole method has been adapted to speed-up the inverse solution process. To rapidly analyze the radiation pattern of electrically large parabolic reflector antenna, the MoM accelerated with MLFMM is proposed [10]-[12]. In [13], it shows excellent agreement of physical optics results in the main lobe and out to several lobes has been found with those of MLFMM accelerated MoM technique. In order to further improve the speed of calculation, it is preferred to combine MoM with physical optics (PO) to analyze reflector antenna problems [14]. For the antenna radiation problems, it is a key to get the gain of main lobe. PO method can provide the main lobe gain with high efficiency. Therefore, it can be used as a promising tool to simulate the radiation pattern of antenna. In [15], PO is used to analyze the radiation pattern of a monopole antenna mounted on an aircraft. In order to analyze the reflector antenna efficiently, [16] applied graphics processing units to PO in computing the radiated fields. In [17], it proposes a new algorithm about multilevel physical optics for the effective evaluation of the wide angle radiation pattern. Then an acceleration technique was presented in [18] to fast evaluate the monostatic radar cross section. In order to get higher gain with limited size, single reflected antenna is replaced by dual reflector antenna. Reference [19] demonstrates MLFMM is applied to accelerate multiple reflection Physical Optics significantly. Recently, multilevel sampling and interpolation of phase-compensated and amplitude-compensated is applied to the double bounce through physical optics [20]. In [21], it is first to use the MLFMM algorithm for internal field calculations, and consider effect of internal shadowing on the factorized version of the field evaluation matrix, without compromising speed and accuracy. Although the double-bounce physical optics is accelerated by the above technology, it is still time-consuming to optimize large aperture antennas, especially in high frequency. It is significant to develop more efficient approach for

dual reflector antenna.

A new DBPO (double bouncing physical optics) technique is proposed to evaluate the radiation pattern of the dual reflector parabolic antenna. It is a novel combination between DBPO and MLFMM. In order to obtain the equivalent current of main reflector high efficiently, the effect of the subreflector's equivalent electric current on the main reflector's equivalent electric current is accelerated by MLFMM. Because of the distance between the main reflector and subreflector is long, we use window function to further accelerate the operation of transfer. Suppose N_1 and N_2 are the number of unknowns on the sub and main reflectors respectively. The computational complexity of computing the bounce between reflectors, that can be reduced from $O(N_1 * N_2)$ to $O(N_1 + N_2)$ by using the new approach.

With the increase of N_1 and N_2 , the efficiency of new method is more evident. Several examples are presented to validate the superior efficiency and accuracy of the proposed method.

II. THEORY AND FORMULATION

A. Physical Optics

The radiation is obtained by the equivalent electric current on the surface of the metallic reflector. The equivalent currents are zero when the surface is not illuminated by incident plane wave, and it has the following expressions in the illuminated area:

$$\vec{J}(\vec{r}') = 2\hat{n} \times \vec{H}^{inc}(\vec{r}'), \quad (1)$$

where \hat{n} is the unit normal vector of the surface at point \vec{r}' , $\vec{H}^{inc}(\vec{r}')$ is the incident magnetic field. The radiation diagram of metallic surface as follows:

The radiation pattern is:

$$\vec{E}(\vec{r}) = -jk_0\eta_0 \left(\vec{\bar{I}} + \frac{1}{k_0^2} \nabla \nabla \right) \iint_S \vec{J}(\vec{r}') G(\vec{r} | \vec{r}') ds, \quad (2)$$

where $\eta_0 = \sqrt{\frac{\mu_0}{\epsilon_0}}$ presents the free space wave impedance, $k_0 = \omega\sqrt{\epsilon_0\mu_0}$ presents the free space wave number.

According to the far field approximation, the Green's function is simplified as follows:

$$G(\vec{r} | \vec{r}') = \frac{e^{-jk|\vec{r}-\vec{r}'|}}{4\pi|\vec{r}-\vec{r}'|} \approx \frac{e^{-jkr}}{4\pi r} e^{jk\vec{r}' \cdot \hat{R}}, \quad (3)$$

where \hat{R} is the unit vector of the observed point in spherical coordinates in terms of the rectangular coordinates system, the expression is:

$$\hat{R} = \sin\theta \cos\phi \hat{x} + \sin\theta \sin\phi \hat{y} + \cos\theta \hat{z}. \quad (4)$$

The radiation field of the reflector antenna is expressed as:

$$\vec{E}(\vec{r}) = -jk_0\eta_0 \left(\vec{\bar{I}} + \frac{1}{k_0^2} \nabla \nabla \right) \iint_S \vec{J}(\vec{r}') \frac{e^{-jkr}}{4\pi r} e^{jk\vec{r}' \cdot \hat{R}} ds'. \quad (5)$$

Only the item of $1/r$ is retained in the far field of radiation, and electric filed intensity is:

$$\vec{E}(\vec{r}) = -jk_0\eta_0 \frac{e^{-jkr}}{4\pi r} \left(\vec{\bar{I}} - \hat{R}\hat{R} \right) \iint_S \vec{J}(\vec{r}') \frac{e^{-jkr}}{4\pi r} e^{jk\vec{r}' \cdot \hat{R}} ds'. \quad (6)$$

where $\vec{\bar{I}}$ represents the dyadic unit vector, and $\hat{R}\hat{R}$ represents the dyadic unit vector of \hat{R} .

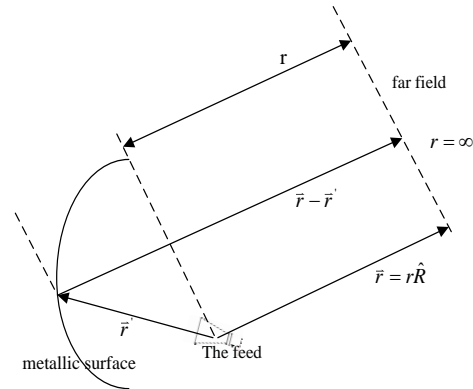


Fig. 1. Radiation of the single reflector antenna in PO.

In Fig. 2, for the dual reflector antenna, it is suitable to apply double bounce physical optics rather than PO. The radiation field of the main reflector is obtained through the equivalent electric current of the subreflector:

$$\begin{aligned} \vec{H}_{sc} &= \iint \vec{J}_s \times \nabla' g dS \\ &= \frac{1}{4\pi} \iint \frac{e^{-jkr_m}}{r_m} (\vec{J}_s \times \vec{r}_m) \left(jk + \frac{1}{r_m} \right) dS \end{aligned}, \quad (7)$$

where dS represents the area of each triangle in subreflector, and \vec{J}_s represents the tangential equivalent electric current of each triangle in subreflector.

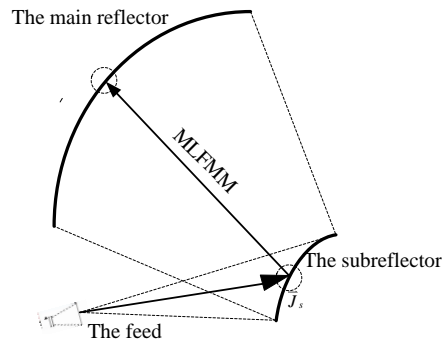


Fig. 2. Dual offset reflector antenna.

B. A novel method based on MLFMM

Triangles are usually used to fit the surface of the object, and $\lambda/10$ is taken as the mesh size. Where λ is the wavelength of the incident wave. It is time-consuming to get the incident field of the main reflector. Due to the fact that the distance between the main reflector and the subreflector is farther than 10λ , where the main reflector regards as the far field for the subreflector. Therefore we speed up the process of (7) through a novel method, which modifies from MLFMM [22]-[24]. All the aggregations happen in subreflector, and all configurations appear in the main reflector. This is different from the MLFMM. In MLFMM, aggregation and configuration are determined by the distance between the groups. If the distance between two groups are close, the contribution of group is obtained by direct numerical calculation. Only the distance between two groups is long, it uses MLFMM to accelerate the contribution. In proposed algorithm, because the group of main reflector and the group of subreflector are far apart, all the contribution are evaluated by MLFMM. Through three processes of aggregation, transfer and configuration in Fig. 3, the acceleration of the computation is achieved. Firstly, the contribution of every source point is aggregated to the center of the corresponding group. In order to simplify the computation, the source point is defined as the center of the meshed triangle in the subreflector. The equivalent electric current of every point is considered as the basic function of corresponding triangle. Secondly, after finishing aggregation, the contribution of group of source point transfers to the group center of observed point. Thirdly, the contribution of observed point's group center is configured to the observed point, and the configuration is the inverse operation of aggregation.

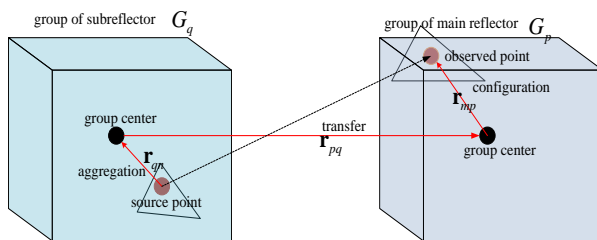


Fig. 3. Principle of accelerating the effect of the subreflector to the main reflector in single level.

The main reflector and the subreflector are surrounded by box through octree grouping. Then the two reflectors are divided into many groups, and (7) is the contribution of the current. The entire solution region is first enclosed in a large group (the red cube at n+1 level in Fig. 4), which is divided into eight smaller groups (the red cubs at n level in Fig. 4). Each sub-

group is then recursively subdivided into smaller sub-groups until the finest group (the yellow cube in Fig. 4) contains a few current elements. The level of groups is determined by the distance between the two elements in MLFMM. In Fig. 4, every group of n-1 level transfers at the n-1 level. This is the operation of transfer. Meanwhile, every group of n-1 level gathers into the n level, which is the father group of n-1 level. This is the operation of aggregation. Then every group of n level is transferred at the n level. Every group of n level gathers into the n+1 level, which is the father group of n level. Above operation is aggregation and transfer, and configuration is reverse of aggregation. Every group of n+1 level is configured to the n level. In MLFMM, the aggregation process starts from the bottom level, and the configuration process starts from the top level.

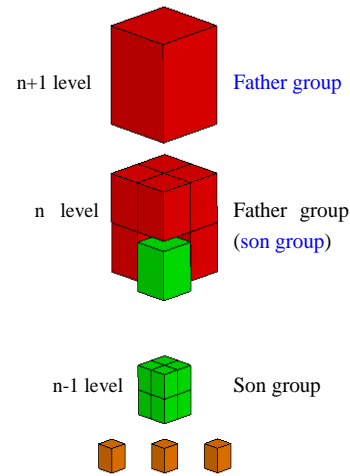


Fig. 4. Multi-level of aggregation, transfer and configuration.

If the distance between the main reflector and the subreflector, satisfying the following condition:

$$\left| \mathbf{r}_{pq}^v \right| > \left| \mathbf{r}_{mp}^v \right| + \left| \mathbf{r}_{nq}^v \right|, \quad (8)$$

Where \mathbf{r}_{pq}^v is orientation that from source group center of subreflector to observed group center of main reflector, and \mathbf{r}_{mp}^v is orientation that from source group center of main reflector to observed group center of main reflector. \mathbf{r}_{nq}^v is orientation that from group center of subreflector to group center of main reflector.

Because the distance between the main reflector and subreflector is far, the main reflector is regarded as the far-field of the subreflector. In this case, the operation of aggregation-transfer-configuration is to accelerate this progress, which solving the equivalent

electric current of main reflector from the equivalent current of subreflector.

The Green's function can be unfolded as:

$$g = \frac{e^{-jk\bar{r}_{mn}^v}}{r_{mn}}, \quad (9)$$

$$= -\frac{jk}{4\pi} \oint e^{-jk \cdot (\bar{r}_{mp}^v + \bar{r}_{qn}^v)} T_L(\bar{k} \cdot \bar{r}^v) d^2k$$

$$\nabla' g = \frac{k^2}{4\pi} \bar{k} \oint e^{-jk \cdot (\bar{r}_{mp} + \bar{r}_{qn})} T_L(\bar{k} \cdot \bar{r}) d^2k, \quad (10)$$

$$T_L(\bar{k} \cdot \bar{r}) \approx \sum_{l=0}^L (-j)^l (2l+1) h_l^{(2)}(k_o r_{pq}) P_l(\bar{r} \cdot \bar{k}), \quad (11)$$

where multipole mode number L is infinite. In order to calculate the $T_L(\bar{k} \cdot \bar{r})$, L is cut off. L has an empirical formula:

$$L = kd + \alpha \log(\pi + kd), \quad (12)$$

$$\alpha = -\log(\varepsilon), \quad (13)$$

$$\beta = 1.8(-\log(\varepsilon))^{2/3}, \quad (14)$$

where d represents the diagonal length of the group and ε represents the precision.

Through transforming the Green's function, (7) is expressed as:

$$\bar{H}_{sc} = \iint \bar{J}_s \times \nabla' g dS'$$

$$= \frac{k^2}{4\pi} \iint \bar{J}_s \times \bar{k} \oint e^{-jk \cdot (\bar{r}_{mp} + \bar{r}_{qn})} T_L(\bar{k} \cdot \bar{r}) d^2k dS', \quad (15)$$

$\bar{J}_s \times \bar{k} e^{-jk\bar{r}_{mp}}$ represents the factor of aggregation, $T_L(\bar{k} \cdot \bar{r})$ represents the factor of transfer and $e^{-jk\bar{r}_{qn}}$ represents the factor of configuration.

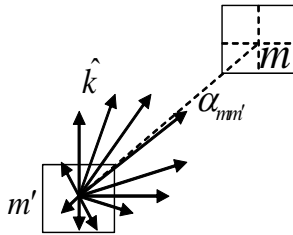


Fig. 5. Sketch map of window function.

In order to accelerate the operation of transfer, we add a window function to the transfer matrix:

$$w_l = \begin{cases} 1 & l \leq J \\ \frac{1}{2} \left[1 + \cos\left(\frac{l-J}{L-J} \pi\right) \right] & l > J \end{cases} \quad (16)$$

In Fig. 5, after the transfer factor multiplied by upper window function, the window function, like a bandpass filter, filters out the area that is not concerned. The transfer component at a certain distance from the center of the group becomes smaller. Because of the long distance between source and observation. Through the window function, we omit many of the angular spectral components that have less influence on the transfer process. Thus this function makes the calculation more efficient.

C. NURBS modeling

The NURBS [25] surface is a bivariate piecewise rational function, which is P order in the direction of u and Q order in the direction of v . The basic expression is as follows:

$$\mathbf{S}(u, v) = \frac{\sum_{i=0}^n \sum_{j=0}^m w_{ij} N_{i,p}(u) N_{j,q}(v) P_{ij}}{\sum_{i=0}^n \sum_{j=0}^m w_{ij} N_{i,p}(u) N_{j,q}(v)}, \quad (17)$$

in which P and Q are the order, m and n are the number of control points in the direction of u and v . $N_{i,p}(u)$ is P cubic B spline basis function, which is obtained by the node vector $U = [u_0, u_1, \dots, u_{n+k+1}]$ according to the de-Boor-Cox recurrence formula. P_{ij} represents the control points of surface, w_{ij} is the weight of every control point:

$$N_{i,0}(u) = \begin{cases} 1 & \text{if } u_i \leq u \leq u_{i+1} \\ 0 & \text{otherwise} \end{cases}, \quad (18)$$

$$N_{i,p}(u) = \frac{u - u_i}{u_{i+p} - u_i} N_{i,p-1}(u) + \frac{u_{i+p+1} - u}{u_{i+p+1} - u_{i+1}} N_{i+1,p-1}(u) \quad (19)$$

The piecewise rational base function is:

$$R_{i,j}(u, v) = \frac{w_{ij} N_{i,p}(u) N_{j,q}(v)}{\sum_{k=0}^n \sum_{l=0}^m w_{kl} N_{k,p}(u) N_{l,q}(v)}. \quad (20)$$

The NURBS expression can be abbreviated as:

$$\mathbf{S}(u, v) = \sum_{i=0}^n \sum_{j=0}^m R_{i,j}(u, v) P_{ij}. \quad (21)$$

As is shown in Fig. 6, we change the model through changing the control points (red points), which are selected by Rhinoceros software. The weight of control points is set to 1.

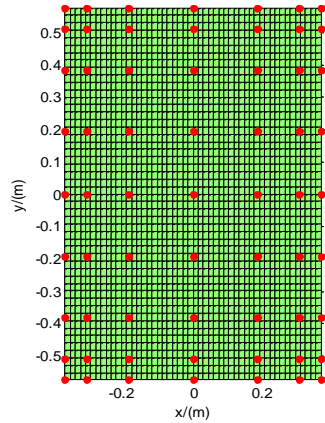


Fig. 6. NURBS fitting plane.

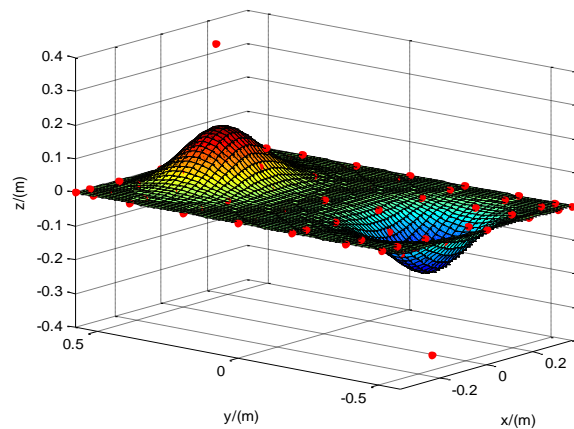


Fig. 7. Change value of two control points in Z coordinate to get the new surface.

In Fig. 6, the x axis represents the direction of V, and the y axis represents the direction of U. The surface around the control point varies with the control point and has no effect on the far curved surface. Through changing 7*9 control points, we can achieve different surface what we want. In Fig. 7, changing the value of two control points in Z coordinate constantly, we will get many surface with different shapes. In the optimization process of the reflector antenna, it has a fixed contour. Only the value of the control point is changed in Z coordinate, the projection shape of the surface in the XOY plane is not affected. Therefore, the outline of the reflector antenna does not have any change. This is why the NURBS modeling is chosen to apply in the shape optimization of the reflector antenna.

III. NUMERICAL RESULTS

The CPU has Intel core Q9500 and 8GB memory. The environment is based on the Fortran MPI.

In Fig. 8, it is the dual offset Cassegrain antenna with primary reflector diameter of 2.5m and rectangular

secondary reflector diameter of 1.08m*1.06m, and the feed adopts the ideal horn feed with the right circular polarization. Since the antenna is a shared antenna, and it should be optimized simultaneously both at the receiving and transmitting frequency. The mesh size is 0.4 times the wavelength of the receiving frequency at 28GHz, and the triangle of the primary reflector with 927395, the secondary reflector with 150785. The phi of simulation is 0 degree and the theta ranges from -5 degree to 5 degree. The tangential plane pattern of DBPO, DBPO with MLFMM at 18GHz is shown in Fig.9, and DBPO and the proposed method is in good agreement in the main lobe, so is the near-sidelobe. The result of FEKO and the proposed method has difference in sidelobe. We pay attention to the main lobe and near-sidelobe in this problem. Therefore the proposed method meet the application requirements.

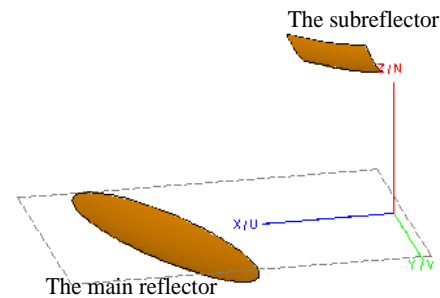


Fig. 8. Model of the dual offset Cassegrain antenna.

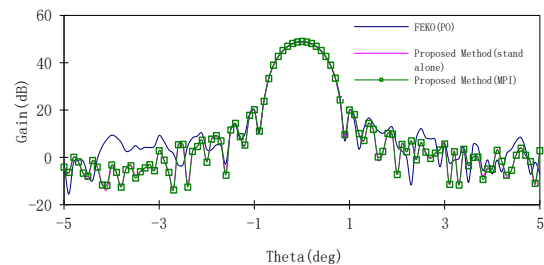


Fig. 9. Radiation pattern of the dual reflector antenna in different methods.

Table 1: Efficiency of different methods

	PO	Proposed Method (Stand-alone)	Proposed Method (MPI with 15 Core)
Time (s)	16214.32	156.84	15.49

The enormous advantage of the proposed method is shown in Table 1. The proposed method is 103.38 times faster than traditional method (DBPO). The presented method combined optimization algorithm applies to optimize the dual reflection antenna, especially for the large aperture antenna.

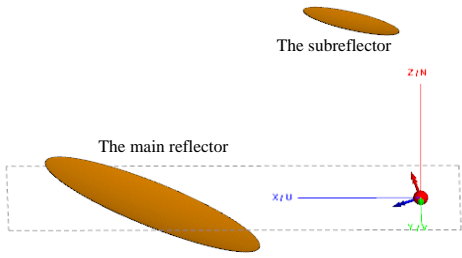


Fig. 10. Model of the dual offset Cassegrain antenna.

In Fig. 10, the diameter of the main reflector is 2.5m, the focal length is 3.74m, and the center offset height is 3.12m. The focal length of the subreflector is 1.456m, and the distance of the hyperbolic vertex is 1.248m. We model the main reflector and subreflector through NURBS, and select 9*9 control points to change the shape of the main reflector and subreflector. The shape of the initial reflector and the coordinates of the control points are shown in Fig. 11.

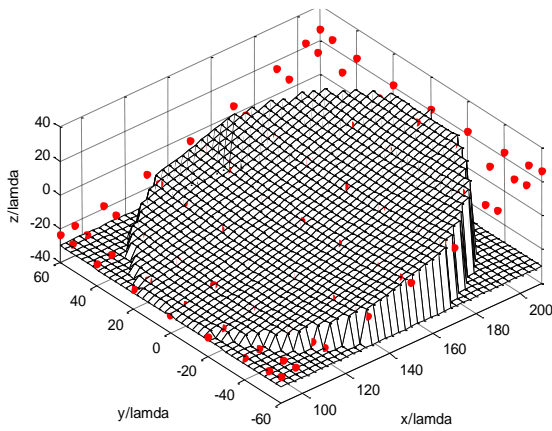


Fig. 11. Initial main reflector and control points.

In Fig. 12 and Fig. 13, the center frequency point of transceiver is 28GHz in Ka band. Since the performance of the 70 beams is approximately similar, it can only be optimized by taking several representative beams at the center and edge. For a high gain narrow beam antenna, we properly take less sampling point to the optimized target area. Here we take 8 sampling points from each edge of the beam and the symmetrical sampling points of equal distance, which guarantee the symmetry of the optimized beam. At the same time, a point is picked up at the center, which reduces the number of the sampling points and prevents the center of the radiation pattern from sinking. The optimization goal is that the directional coefficient of 0.8 degree beam is greater than 45dB.

By optimizing the shape of the reflector, we achieve the radiation pattern which meets 45dB as shown in Fig. 13.

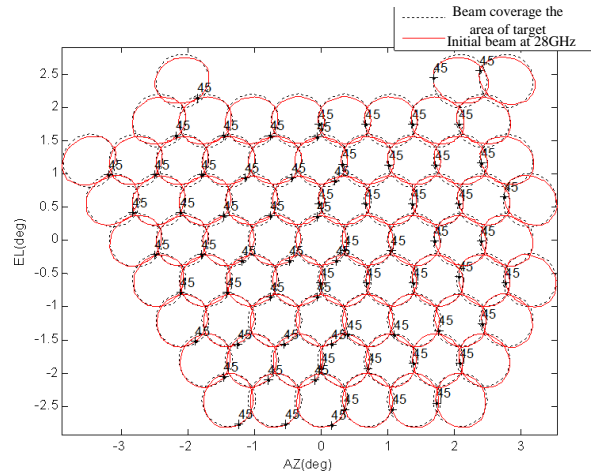


Fig. 12. Isoline pattern of the initial beam at the frequency of 28GHz.

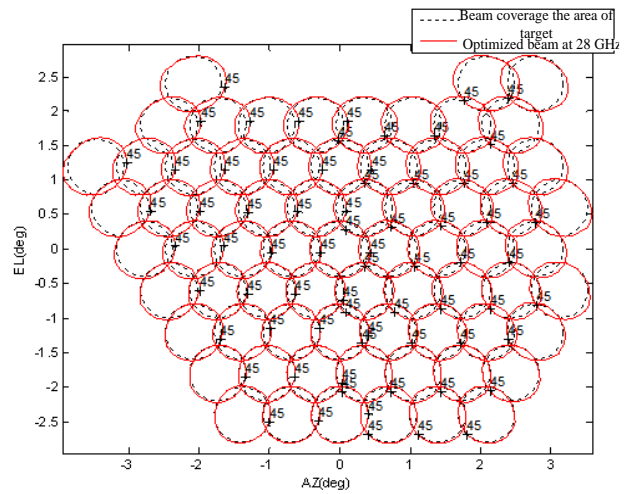


Fig. 13. Isoline pattern of the optimized beam at the frequency of 28GHz.

VI. CONCLUSION

An innovative MLFMM-DBPO approach for calculating the radiation pattern of the dual reflector antenna is proposed in this work. The new method reduces the computational complexity and expedites the simulation of antenna with DBPO fundamentally. It is significant for optimizing the shape of large aperture antenna and analyzing the radiation of large electrical objects, such as the satellite antenna. According to the numerical results, the new algorithm is more efficient than traditional DBPO with encouraging accuracy.

ACKNOWLEDGMENT

This work was supported in part by Natural Science Foundation of 61701232, 61431006, 61771246, Jiangsu Province Natural Science Foundation of BK20170854, the China Postdoctoral Science Foundation

of 2017M620861.

The Authors are with the Department of Communication Engineering, Nanjing University of Science and Technology, Nanjing 210094, China. (E-mail: zihe@njust.edu.cn).

REFERENCES

- [1] I. Aghanejad, H. Abiri, and A. Yahaghi, "Design of high-gain lens antenna by gradient-index metamaterials using transformation optics," *IEEE Transactions on Antennas & Propagation*, vol. 60, pp. 4074-4081, 2012.
- [2] D. W. Boeringer and D. H. Werner, "Particle swarm optimization versus genetic algorithms for phased array synthesis," *IEEE Transactions on Antennas and Propagation*, vol. 52, pp. 771-779, 2004.
- [3] D. Pozar and D. Schaubert, "Scan blindness in infinite phased arrays of printed dipoles," *IEEE Transactions on Antennas and Propagation*, vol. 32, pp. 602-610, 1984.
- [4] A. Molaei, J. H. Jueas, and W. J. Blackwell, "Interferometric sounding using a metamaterial-based compressive reflector antenna," *IEEE Transactions on Antennas & Propagation*, vol. 66, pp. 2188-2198, 2018.
- [5] M. Albani, G. L. Cono, and R. Gardelli, "An efficient full-wave method of moments analysis for RLSA antennas," *IEEE Transactions on Antennas & Propagation*, vol. 54, pp. 2326-2336, 2006.
- [6] C. H. Schmidt and T. F. Eibert, "Multilevel plane wave based near-field far-field transformation for electrically large antennas in free-space or above material halfspace," *IEEE Transactions on Antennas and Propagation*, vol. 57, pp. 1382-1390, 2009.
- [7] T. F. Eibert and C. H. Schmidt, "Multilevel fast multipole accelerated inverse equivalent current method employing rao-wilton-glisson discretization of electric and magnetic surface currents," *IEEE Transactions on Antennas and Propagation*, vol. 57, pp. 1178-1185, 2009.
- [8] F. T. Wu, "Design of a new millimeter wave paraboloidal reflector antenna using MLFMM," *IEEE Transactions on Antennas and Propagation*, 2014.
- [9] Z. Zhao, L. Li, and J. Smith, "Analysis of scattering from very large three-dimensional rough surfaces using MLFMM and ray-based analyses," *IEEE Antennas & Propagation Magazine*, vol. 47, pp. 20-30, 2005.
- [10] M. Chen, R. S. Chen, and X. Q. Hu, "Augmented MLFMM for analysis of scattering from PEC object with fine structures," *Applied Computational Electromagnetics Society Journal*, vol. 26, pp. 418-428, 2011.
- [11] T. F. Eibert, "Modeling and design of offset parabolic reflector antennas using physical optics and multilevel fast multipole method accelerated method of moments," *IEEE Multitopic Conference*, 2006.
- [12] A. Miura and Y. Rahmat-Samii, "Spaceborne mesh reflector antennas with complex weaves: Extended PO/periodic-MoM analysis," *IEEE Trans. Antennas Propag.*, vol. 55, pp. 1022-1029, 2007.
- [13] M. Ariasacuna and T. Jost, "Physical optics analysis of the radiation pattern of an antenna mounted on an aircraft," *2015 9th European Conference on Antennas and Propagation (EuCAP)*, 2015.
- [14] O. Borries, B. J. Dammann, E. Rgensen, et al., "Reflector antenna analysis using physical optics on graphics processing units," *The 8th European Conference on Antennas and Propagation (EuCAP 2014)*, 2014.
- [15] C. Letrou and A. Boag, "Generalized multilevel physical optics (mlpo) for comprehensive analysis of reflector antennas," *IEEE Transactions on Antennas and Propagation*, vol. 60, pp. 1182-1186, 2012.
- [16] Y. An, D. Wang, and R. Chen, "Improved multilevel physical optics algorithm for fast computation of monostatic radar cross section," *IET Microwaves Antennas & Propagation*, vol. 8, pp. 93-98, 2014.
- [17] D. P. Xiang and M. M. Botha, "Acceleration of multiple reflection physical optics scattering analysis with the MLFMM," *2016 10th European Conference on Antennas and Propagation (EuCAP)*, 2016.
- [18] M. Roudstein, Y. Brick, and A. Boag, "Multilevel physical optics algorithm for near-field double-bounce scattering," *IEEE Transactions on Antennas & Propagation*, vol. 63, pp. 5015-5025, 2015.
- [19] D. P. Xiang and M. M. Botha, "Acceleration of multiple reflection physical optics scattering analysis with the MLFMM," *European Conference on Antennas & Propagation*, 2016.
- [20] F. T. Wu, "Design of a new millimeter wave paraboloidal reflector antenna using MLFMM," *Proceedings of 2014 3rd Asia-Pacific Conference on Antennas and Propagation*, 2014.
- [21] J. Cao, S. F. Tao, and R. S. Chen, "An efficient solution for volume integral equation based on meshfree scheme," *IEEE Antennas & Wireless Propagation Letters*, vol. 14, pp. 1618-1621, 2015.
- [22] D. Z. Ding, R. S. Chen, and Z. H. Fan, "A novel hierarchical two-level spectral preconditioning technique for electromagnetic wave scattering,"

IEEE Transactions on Antennas & Propagation, vol. 56, pp. 1122-1132, 2008.

- [23] J. Yan, J. Hu, and Z. Nie, "Calculation of the physical optics scattering by trimmed NURBS surfaces," *IEEE Antennas & Wireless Propagation Letters*, vol. 13, pp. 1640-1643, 2014.



Jun Li was born in Taizhou, China. He received the B. S. degree in Optical Engineering from the School of Electrical Engineering and Optical Technique, Zijin College of Nanjing University of Science and Technology, Nanjing, China, in 2013. He is currently pursuing his Ph.D. degree in Electronic Engineering at Nanjing University of Science and Technology.

The interest of his research are about antennas, high frequency method and computational electromagnetics.

Chunbang Wu received the B.S. degree in Radio Propagation and Antenna of Wuhan University in 1992. He received the Master's degree in Insitut national de polytechnique-Toulouse. He mainly researches in space antenna technology and satellite payload technology.